Rev. Roum. Sci. Techn.– Électrotechn. et Énerg.
Vol. **67**, *4*, pp. 409–415, Bucarest, 2022

CURVED DIPOLAR ELECTROMAGNET, NUMERICAL MODELING AND DESIGN

ION DOBRIN[1], DAN ENACHE[1], GEORGE DUMITRU[1], MIHAI GUTU[1], STEFANIA ZAMFIR[1], RADU PINTEA[1]

Keywords: Curved electromagnet; Dipole; Finite element analysis; Magnetic field; Design.

A conceptual design for a normal conducting curved magnet, which, after optimization, is the current best design that achieves the requirements for the generated magnetic field, is proposed. The primary purpose of the analytical effort, the results of which are presented, is to develop a viable engineering design satisfying requirements to the parameters of the generated magnetic field and the electromagnet functional and structural ones. The work includes the proposed conceptual approaches, modeling analysis of the generated magnetic field, and the technical design for the conductor and winding pack parameters. The magnet's structural design, the winding's heating, the designed parameters of the electromagnet cooling system, and the power supply parameters are also provided.

1. INTRODUCTION

Electromagnets intended for use in particle accelerators [1, 2] and which deflect the flow of electrically charged particles to force them to move in a curvilinear or circular trajectory are usually rectilinear, the deviation from the initial direction of the particles being practically given by the length and the width of the dipole magnetic field area generated in the dipole electromagnets. Of course, the number of electromagnets needed in an accelerator is given by the radius of the acceleration trajectory and, therefore, by the particle flow's final energy.

There are two ways to reach higher acceleration energies: either by increasing the accelerator radius and implicitly the number of linear electromagnets needed with a direct impact on the value of the initial investment or increasing the value of the magnetic field induction used, which requires superconducting electromagnets with significant impact on the initial investment.

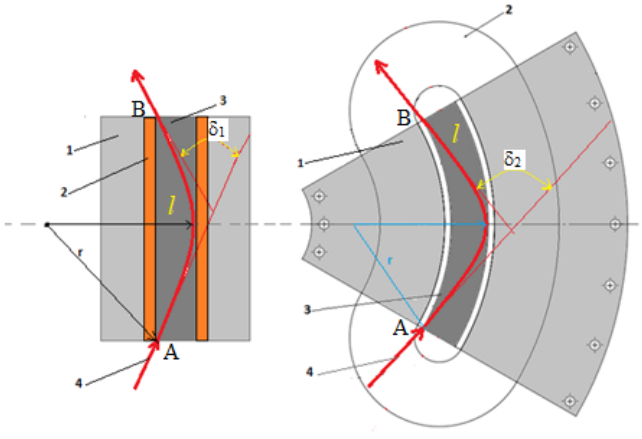

(a) (b)

Fig. 1 – Illustration of the deviation of electrically charged particles in the linear dipole magnetic field (a) and in the curved dipole magnetic field (b).

An intermediate solution is to increase the deviation of the particles in the magnetic field area by changing the geometric shape of the dipole electromagnets from linear to curvilinear. Thus, the concept of curved dipole electromagnet appears, having the shape of a circle segment or circular sector (Fig. 1,b), which gives the accelerated particles, a considerably increased deflection angle ($\delta_2>\delta_1$), for the same induction of the magnetic field and an effective length of the field area, identical. Such electromagnets [3, 4] are more difficult to achieve. Still, the general advantages are essential: reducing the number of deflection electromagnets by reducing the radius of curvature of the accelerator and thus reducing investment costs. In recent years, attempts have been made to replace conventional superconducting electromagnets (made with NbTi and Nb_3Sn) [5] with high-temperature superconductor (HTS) dipole electromagnets [6, 7].

According to Fig. 1, we have the following notations: 1- Iron yoke; 2- Normal conductive winding; 3- Dipolar magnetic field area; 4- Movement trajectory of electrically charged particles.

The trajectory of electrically charged particles in a magnetic field with induction B (when B is perpendicular to the plane of the trajectory determined by two vectors **r** and **p**), is a circular arc whose radius of curvature r results from the equilibrium condition of the particle when moving on the circular trajectory and is given by the relation:

$$r = \frac{p}{qB}, \tag{1}$$

where p [GeV/c] is the particle momentum, q [C] is the particle charge, and B [T] is the magnetic flux density component perpendicular to the plane of the trajectory.

The change of direction of the electrically charged particles, due to the motion in the magnetic field area, is highlighted by the deviation angle δ [radians], which is given by the relation:

$$\delta = \int_0^l \frac{dl}{r}, \tag{2}$$

Using relation (1) yields

$$\delta = \frac{q}{p}\int_0^l Bdl, \tag{3}$$

where the integral is calculated along the entire length of the particle trajectory (l – between points A and B, shown in Fig. 1).

Thus, the momentums (p) of the particles can be measured by determining their deviation angle δ in the magnetic field and by calculating the field integral along the trajectory:

$$p \cong \frac{k}{\delta}\int_0^l Bdl, \tag{4}$$

[1] National Institute for Research and Development in Electrical Engineering ICPE-CA, 313 Splaiul Unirii, District 3, Bucharest – 030138, Romania, E-mail: ion.dobrin@icpe-ca.ro, dan.enache@icpe-ca.ro, george.dumitru@icpe-ca.ro, mihai.gutu@icpe-ca.ro, zamfir.stefania@icpe-ca.ro, radu.pintea@icpe-ca.ro

where $k = 0.2998$ is a constant result of the transformation of physical units [2].

Since the acceleration of particles takes place at relativistic speeds, the energy, E [GeV] of the particles can be determined [8]:

$$E = pc = c\frac{k}{\delta}\int_0^l Bdl \quad (5)$$

where and c [m/s] the speed of light in vacuum.

Thus, dipole electromagnets can be used as energy spectrometers, highlighting the energy spectrum of accelerated particles. The curved dipole electromagnets will have a higher energy resolution due to the much more pronounced deviation in the magnetic field and, consequently, a better energy resolution.

2. CONCEPTUAL MODEL OF THE CURVED DIPOLAR ELECTROMAGNET

Figure 2 shows the conceptual model of a curved dipole electromagnet. Compared to the "straight" dipole magnet model, this ensures a more significant deviation of the charged particle beam over a given straight distance (length of the magnetic field area).

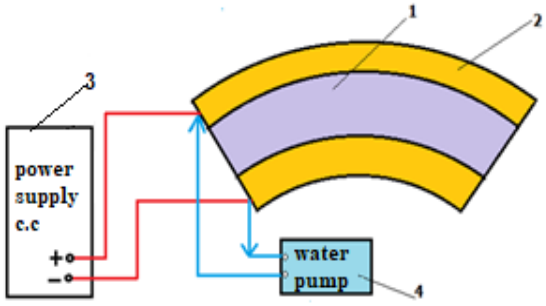

Fig. 2 – Conceptual model of the curved dipole magnet.

The conceptual model of the curved dipole magnet represented in Fig. 1 has the following components: iron yoke (1), normal conductive winding (2), power supply (3), water cooling circuit (4). Figure 3 shows a 3D CAD image of the curved dipole magnet, which highlights more strongly the two parts of the electromagnet: the iron yoke (1) and the two normal conducting coils (2).

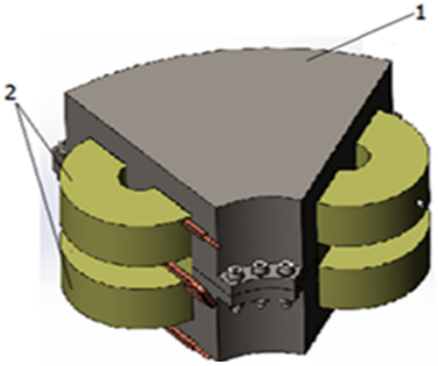

Fig. 3 – 3D CAD general view of the curved dipole.

2.1. THE IRON YOKE OF THE MAGNET

It acts as a magnetic circuit for the dipole magnet. It has the shape of a circle sector and ensures the support of the normal conductive winding in addition to the area of a uniform magnetic field (Figs. 4 and 5).

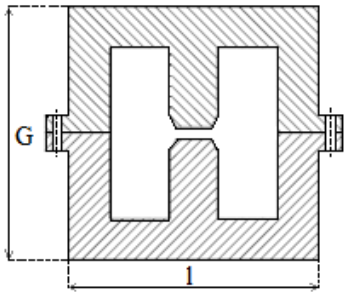

Fig. 4 – Drawing cross-sectional view of the iron yoke

As shown in Fig. 4, the dipole magnet has an “H” type section. The uniform magnetic field is between the magnet's poles (central area).

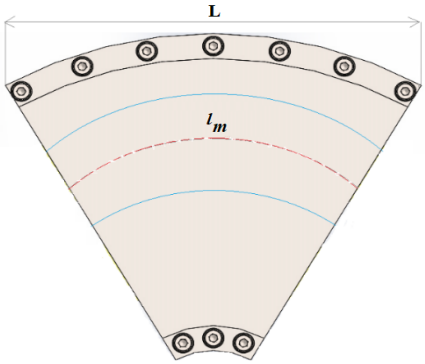

Fig. 5 – 2D CAD view of the iron yoke- upper side.

Figure 5 shows the 2D CAD image of the iron yoke indicating the delimitation of the poles (blue lines) and the median line l_m (red) of the magnetic field area.

Table 1

Iron yoke characteristics

No.	Characteristics	Value
1	Maximum length - L (mm)	330
2	Width - l (mm)	230
3	Thickness - G (mm)	110
4	Medium length magnetic field area - l_m	275
5	Mass (kg)	26

2.2. CURVED DIPOLE MAGNET WINDING

The winding will be made of copper conductor and cooled with water. In this respect, the conductor is provided with a central channel for circulating cooling water. Figure 6 shows the type of copper conductor used in the winding.

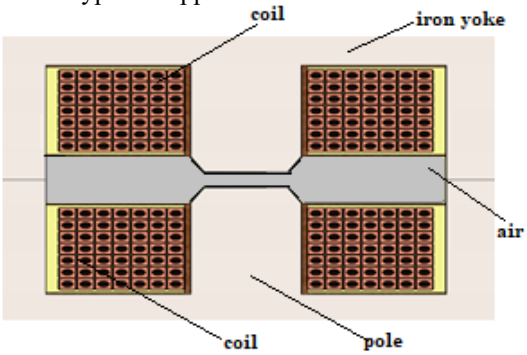

Fig. 6 – 2D CAD view of the curved dipole magnet winding.

The winding structure is special due to the curved shape

required. The winding has 7 layers and 7 turns per layer; 49 turns/winding.

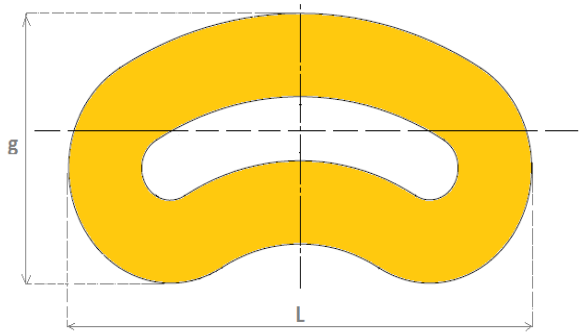

Fig. 7 – The shape of the curved dipole magnet winding.

The characteristics of the electromagnet winding are presented in Table 2.

Table 2.
Winding characteristics

No.	Characteristics	Value
1	Copper conductor cross-section	8.5 x 12.8 mm^2
2	Length (L)	340 mm
3	Width (l)	154 mm
4	Height (g)	85 mm
5	Turns/coils	49

2.3. DC POWER SUPPLY

The electromagnet power supply is a c.c. which can supply currents in the range 0 – 1000 A, at a maximum of 10 V. In the case of these sources, the stability of the current supplied is very important. This stability implies the stability of the generated magnetic field.

2.4. OUTPUT PARAMETERS OF THE POWER SUPPLY

The dc power supply is TDK-Lambda type GSP 10-1000. The constant output voltage, at various values in the range 0-10 V dc with a stability of 0.01 % of rated output voltage and a temperature coefficient of 50 ppm/°C.

Output current with the availability of any value in the range 0-1000 A dc, under the conditions (load regulation) of 0.08% of rated output current and a temperature coefficient of 100 ppm/°C.

2.5. COOLING CIRCUIT

The cooling of the electromagnet is done with the help of a closed-circuit water-cooling system. The circuit comprises a pump for raising and maintaining the pressure in the circuit, a water cooler, and the elements for monitoring the inlet/outlet temperature, the inlet/outlet pressure, and the water flow in the circuit. Thus, the electromagnet has stable conditions of constant cooling, keeping the operating temperature within predetermined limits (40-60 °C). Cooling water is deionized to avoid deposits on the cooling path and alter the cooling parameters over time. The system allows the supply of cooling water of the electromagnet at a variable flow of 3-10 l/min and an inlet pressure of 6 – 15 bar, sufficient to ensure a performance cooling in the thermal conditions mentioned above.

3. NUMERICAL MODELING

3.1. MATHEMATICAL MODEL

The magnetic field problem is solved for the steady state, defined by:

magnetic circuit law

in iron

$$\nabla \times \mathbf{H} = \sigma \mathbf{v} \times \mathbf{B}, \tag{6}$$

the rest of the computing fields

$$\nabla \times \left(\mu_0^{-1}\mu_r^{-1}\mathbf{B}\right) = 0, \tag{7}$$

magnetic flux law

$$\nabla \cdot \mathbf{B} = 0 \Rightarrow \mathbf{B} = \nabla \times \mathbf{A}, \tag{8}$$

where **H** [A/m] is the intensity of the magnetic field, **B** [T] is the magnetic induction, and **A** [T/m] is the magnetic vector potential.

The mathematical model is closed by the magnetic insulation condition:

$$\mathbf{n} \times \mathbf{A} = 0 \tag{9}$$

3.2. NUMERICAL MODELING RESULTS

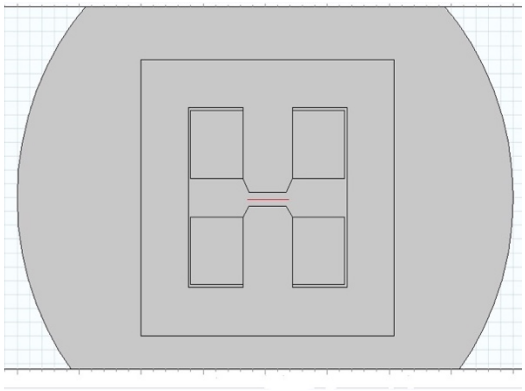

Fig. 8 – Computational domain

Figure 8 shows the computational domain used to model the dipole using [9]. It consists of air, coil, and iron domains. The dipole characteristics are:

conductor type: 7x6 mm with a central hole of 4 mm diameter;
wire material: copper OF (oxygen-free);
number of turns N = 49 / coil;
maximum magnetic flux density: B = 1.51 T;
maximum current used: I = 248 A;
filling factor = 0.74.

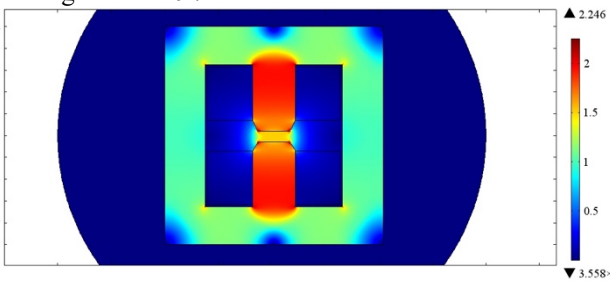

Fig. 9 – Magnetic flux density – color map

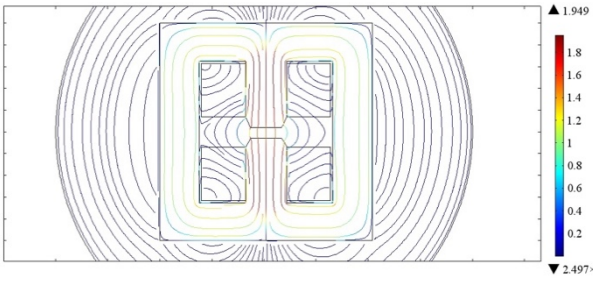

Fig. 10 – Magnetic flux density – field lines

Figures 9 and 10 show the magnetic flux density through a color map through field lines representations.

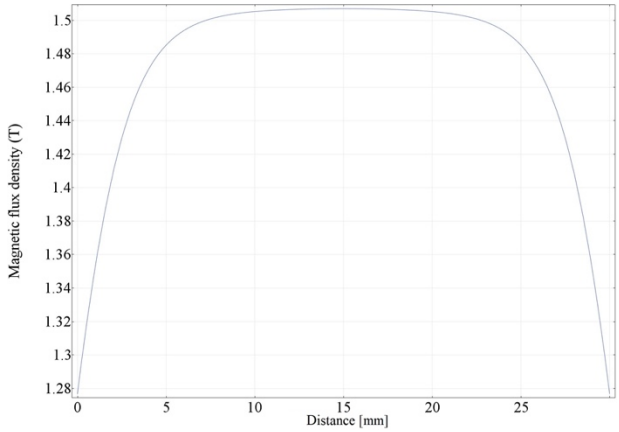

Fig. 11 – Magnetic field in the air gap

The values of the magnetic flux density were calculated along the midline between the two poles and shown in the graph of Fig. 11. The magnetic flux density has a maximum value in the center of the air gap of 1.51 T (along the red line from Fig. 8).

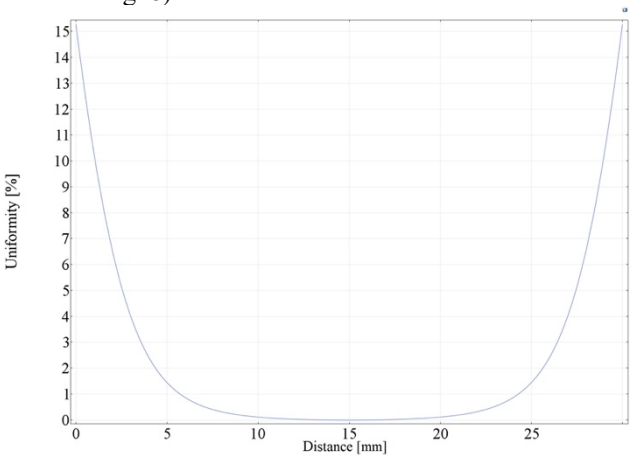

Fig.12 – Non-uniformity of the magnetic field in the air gap area

The variation of the non-uniformity of the magnetic field in the air gap area was studied (along the red line from Fig. 8). The results are shown in Fig. 12.

A non-uniform magnetic flux density of the magnetic field generated in the air gap (dB/B) is obtained, less than 0.5% in a range of 12 mm from the central area of the air gap, which decreases to 0.2 % over a range of 10 mm around the central point of the air gap.

4. ELECTROMAGNET DESIGN

4.1. WINDING AND THE REQUIRED CURRENT COMPUTING

Ampere's law, the magnetic circuit specific to our electromagnet, will be used to calculate the required winding and current. As a model, Fig. 13 schematically presents the type “H” electromagnet in cross-section.

Applying Ampere's law to the magnetic circuit of the electromagnet represented in Fig. 13., we will obtain for the calculation of the winding:

$$NI = \oint_{l_{Fe}} \mathbf{Hdl} \,. \tag{10}$$

Using the eq. (10) to the magnetic circuit from Fig.13, yields:

$$NI = \frac{B_{Fe}}{\mu_0 \mu_r} l_{Fe} + \frac{B_{gap}}{\mu_0} g \,. \tag{11}$$

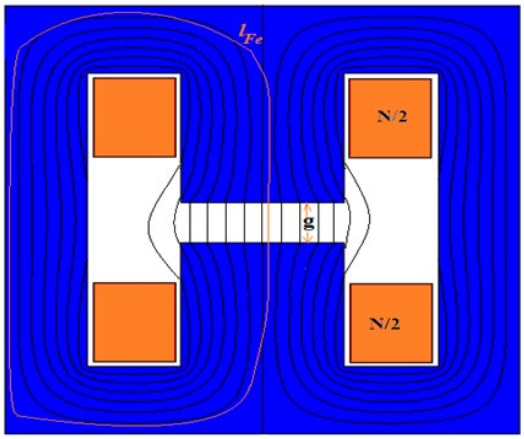

Fig. 13 – Electromagnet type "H" - Ampere's law.

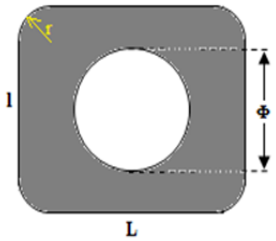

Fig.14 – Section and dimensions for copper conductor

Since $\mu_r \cong 4000$ for iron, we will get:

$$\frac{B_{Fe}}{\mu_0 \mu_r} << \frac{B_{gap}}{\mu_0} \,. \tag{12}$$

Thus,

$$NI \cong \frac{B_{gap}}{\mu_0} g \,, \tag{13}$$

or,

$$NI = \frac{B_{gap}}{\eta \mu_0} g \,, \tag{14}$$

where the "efficiency" of the magnet was denoted by η and is given by the relation:

$$\eta = \frac{1}{1 + \frac{1}{\mu_r} \frac{l_{Fe}}{g}} \,, \tag{15}$$

and g [m] is the height of the air gap, B_{gap} [T] is the magnetic flux density of the magnetic field between the poles of the magnet, N is the total number of turns, and I [A] is the intensity of the electric current used. It will result in $\eta = 0.96$; in our case, the gap has a height of $g = 20$ mm. Starting from the maximum desired value of the induction, the magnetic field in the air gap, $B_{gap} = 1.51$ T, will result in a required winding $NI = 24.620$ A. Choosing a total number of turns $N = 49 \times 2 = 98$ turns, will result in the maximum value of the required current: $I_m = 251$ A.

4.2. CONDUCTOR SIZING

In the case of water cooling, the usual current density used is $J = \leq 10$ A/mm^2.

To calculate the current density, the following expression was used: $J = I_m / S_c$, where S_c is the cross-sectional area

of the conductor used.

Choosing a value of 10 A/mm^2 for J will result in a minimum conductor cross-section: $S_c \approx 25.10$ mm^2. A copper conductor with an internal cooling channel was chosen to make the winding, shown in Fig. 12. and has the following characteristics: L = 7 mm; l = 6 mm; and Φ = 4 mm, the diameter of the central cooling channel. It follows that the relationship gives the useful section of the chosen conductor:

$$S_{cond} = S_{dr} - S_{\Phi} - 4S_c, \quad (16)$$

where S_{dr} is the cross-section area of the conductor (ideally rectangular), S_Φ is the area of the inner circular channel, and S_c is the area of a rounded "corner" of the rectangle, with a radius of r = 1 mm. An effective conductor area will result: S_{cond} = 26.33 mm^2, corresponding to the maximum current used, a maximum current density J = 8.92 A/mm^2. For this value of *J, an efficient cooling system of the conductor is necessary* during the operation of the electromagnet so that the winding does not overheat.

4.3. WINDING SIZING

A 7-layer structure was chosen for the winding, each layer having 7 turns. Thus, the total number of turns for a coil is N_{coil} = 49 turns.

For the realization of the coil shown in Fig. 15, an insulation layer of 0.25 mm thickness was considered. In this case, the height h and the thickness G of a coil are h = 52.5 mm and G = 45.5 mm.

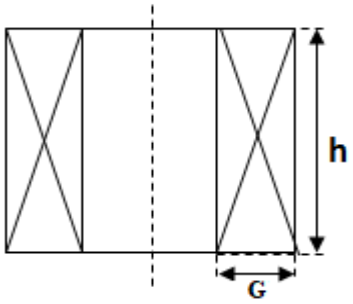

a. Schematic representation of a coil

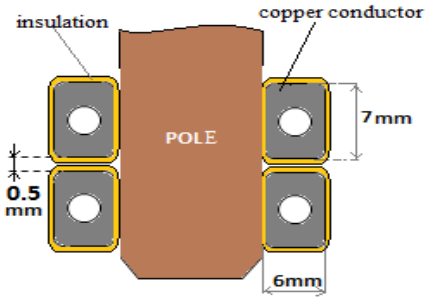

b. Winding – detail.

Fig.15 – Dipole electromagnet coil.

Considering the number of turns of a coil N_b, their distribution, and the general shape of the coil (according to Fig. 15), the total length of the conductor will be l_c = 32.42 m.

Thus, the electrical resistance of the winding is:

$$R_b = \rho_c \frac{l_c}{S_{cond}}, \quad (17)$$

where the resistivity of the chosen copper (OF) for the realization of the winding has the following value ρ_c = 1.7 ·10^{-8} Ωm, and l_c and S_{cond} are the length and the area of the effective cross-section of the copper conductor. As l_c = 32.42 m and S_{cond} has already been calculated in the previous section, a value R_b = 20.94 mΩ will result in coil resistance.

The electrical resistance of the dipole will be $R_D = 2R_b$ = 41.88 mΩ. Thus, the maximum power consumed by the dipole is $P_D = R_D I^2$ = 2646 W.

4.4. WINDING HEATING AND COOLING

The winding of the dipole electromagnet will be subjected to accelerated heating under the conditions of Joule dissipation of a considerable electrical power of a maximum of 3.78 kW. For this reason, a copper conductor with a central channel was chosen for the circulation of cooling water (Fig. 14). The central channel, with a diameter of 4 mm, allows the forced circulation of water at a flow rate that ensures a "working" temperature of the winding of about 60 °C. The cooling water has a closed circuit evacuating the heat produced by the winding to an external cooler (Fig. 16), which brings the water temperature back to a value close to the room (25 °C).

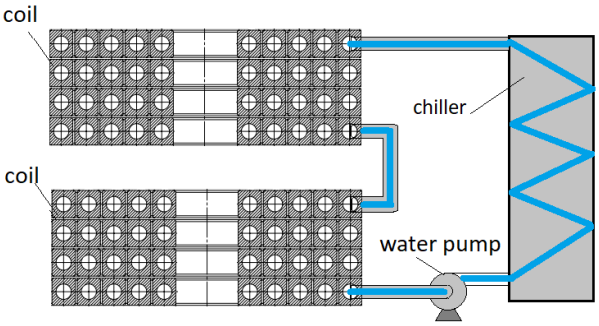

Fig. 16 – Cooling circuit for the electromagnet

The heating of the copper coil will be given by the Joule heat produced, according to the well-known relation:

$$Q = R_b I^2 \Delta t \quad (18)$$

where Q [J] is the amount of heat produced by Joule heating; R [Ω] is the electrical resistance of the conductor; I [A] is the electric current intensity; and Δt [s] is the duration of the presence of electric current.

To evaluate the heating of the copper coil, the following simplifying hypotheses were made:

- the electrical resistivity of copper is constant in the relatively short range of temperature variation (20 - 70 ºC);
- the specific heat of copper is constant in the considered thermal range (20 -70 ºC);
- heating in adiabatic conditions.

Under these conditions, the copper coil will heat up by taking over the Joule heater, according to the equation:

$$Q = m_{cu} c_{cu} \Delta T, \quad (19)$$

where mC_u [kg] is the mass of the copper winding; c_{Cu} [J/KgK] is the specific heat of copper at 25 ºC, and ΔT [ºC] is the increase of the winding temperature.

The winding characteristics are as follows: $m_{Cu} = l_{Cu} d_{Cu}$, where d_{Cu} [Kg/m] is the linear density of the copper conductor. For d_{Cu} = 0.256 Kg/m [10], it results in m_{Cu} = 8.30 kg/coil.

By combining the relations (18) and (19), we obtain the expression of the increase of the temperature of the copper

coil as a function of the duration ΔT of the action of the electric current:

$$\Delta T = \frac{Q}{m_{cu} c_{cu}} = \frac{R_b I^2 \Delta t}{m_{cu} c_{cu}}. \quad (20)$$

The value considered for the specific heat of copper is c_{Cu} = 385 J/kgK [4].

Applying the relation (20) for various values of current and various durations of time, we obtain the temperature increases for the electromagnet winding, which are presented in Fig.14.

Knowing the equation of heating a quantity of fluid:

$$Q = m_a c_a \Delta T, \quad (21)$$

where Q [J] is the amount of heat taken, m_a and c_a, the specific mass and heat of the water, and ΔT, the increase in temperature of the coolant (water).

Because heat transfer from winding to water is a time-dependent process, the heat transfer equation will be:

$$\frac{dQ}{dt} = c_a \Delta T \frac{d}{dt} m_a, \quad (22)$$

$$m_a = \rho_a V_a = \rho_a S_a x, \quad (23)$$

where ρ_a is the water density, V_a [m^3] is the volume occupied by the respective water mass, S_a – the section of the cooling channel and x is the length occupied by the volume of water in the cooling channel. Consequently,

$$\frac{dQ}{dt} = q = c_a \Delta T \rho_a S_a v_a, \quad (24)$$

where $v_a = dx/dt$ is the water circulation speed through the channel. Under these conditions, the water flow is:

$$D_a = S_a v_a. \quad (25)$$

The expression for q is:

$$q = c_a \rho_a D_a \Delta T. \quad (26)$$

We can thus obtain the expression of the increase of the cooling water temperature:

$$\Delta T = \frac{q}{c_a \rho_a D_a}, \quad (27)$$

as $q = P$ [W] is the Joule power produced by the winding and taken over by the cooling water, the flow required to extract the amount of heat P (thermal power) is:

$$D_a = \frac{P}{c_a \rho_a \Delta T}. \quad (28)$$

The calculations were performed for ΔT = 50 ° C *versus* 25 ° C starting temperature.

The final winding temperature is given by

$$T_f = T_i + \frac{P}{c_a \rho_a D_a}. \quad (29)$$

Using the relation (29) the variation of the winding temperature was numerically evaluated according to its cooling water flow. Thus, the final temperatures were calculated for different values of the consumed electric power (Joule), corresponding to the currents I = 100 A; 150 A; 200A, 250 A, and 300 A. The results are shown in Fig. 17. The analysis of the results presented in Fig. 17 yield:

- without any cooling, the winding temperature increases practically indefinitely to very high values (~ 10^2 - 10^3 K), depending on the operating time;
- it is not recommended to maintain the current without proper cooling for longer intervals than 100-150 s, to avoid irreversible damage to the electromagnet winding;
- efficient cooling of the winding is required by using circulating water under pressure.

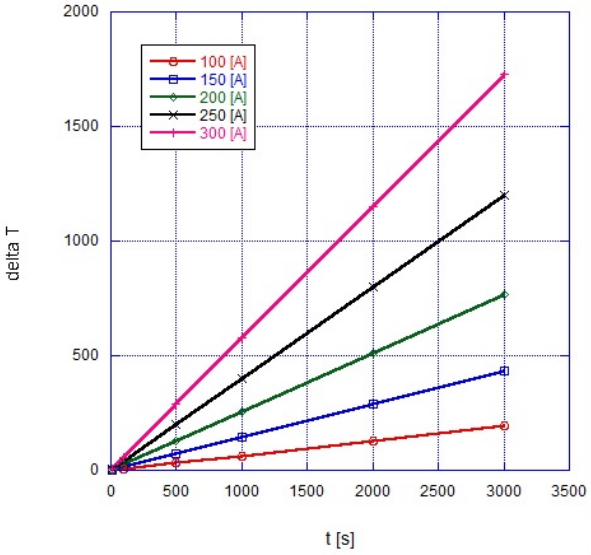

Fig. 17 – The increase in temperature of the electromagnet winding depending on the supply time

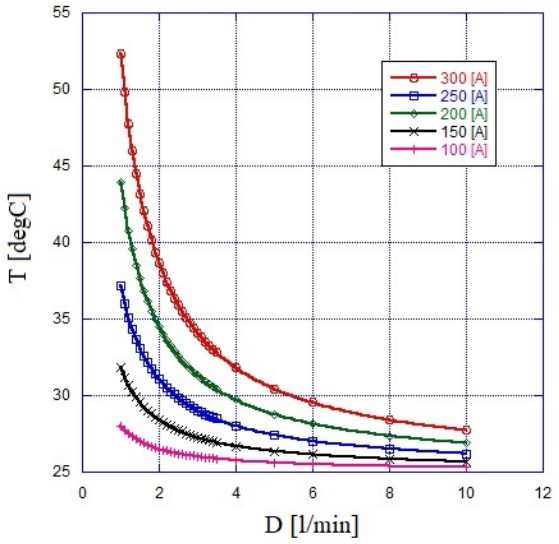

Fig. 18 – Water cooled coil temperature calculation.

From the analysis Fig. 18, it results that a flow rate of 1-3 l / min or more, for the maximum current used of 250 A, is sufficient to keep the winding temperature below the value of 50 ° C.

5. CONCLUSIONS

A conceptual model of curved, normally conductive dipole electromagnet was presented, intended for the accentuated deviation of electrically charged and accelerated particles for applications in nuclear physics and nuclear medicine (hadron therapy). The geometric parameters and the advantages of the curved electromagnet compared to the straight one was

analyzed. By using the FEM analysis to the approached physical model, the parameters of the generated magnetic field were analyzed, obtaining a maximum value of the induction of the magnetic field on the median line of the magnet of $B = 1.51$ T and a transversal non-uniformity of the magnetic field $dB/B = 0.5$ % within 12 mm of the central area of the air gap, which decreases to 0.2% within an area of 10 mm around the central point of the air gap.

The calculation of the sizing of the electromagnet winding, taking into account the laws of electromagnetism, which generate the induction of the maximum field of 1.50 T in the gap, had led to the following values: a copper conductor was chosen with a central cooling channel of 4 mm diameter, with dimensions 7 x 6 mm^2, a conductor that allows a maximum current of 251 A, for a maximum current density of $J = 8.92$ A/mm^2. The winding required to produce the maximum magnetic field led to 49 turns/coil, distributed in 7 layers and 7 turns/layer. The electrical resistance of such a winding will be 41.88 mΩ, requiring a maximum consumed electrical power of 2.646 W.

This power produces a Joule heating of the winding proportional to the duration of the electromagnet operation, the heat that will be evacuated through the cooling system with circulating water through the cooling channel of the conductor. We evaluated numerically for various values of the supply current of the electromagnet the evolution of the winding temperature as a function of time, which shows a continuous thermal increase in the absence of adequate cooling. An algorithm for calculating the water cooling of the winding was also developed, and the final cooling temperature of the winding was numerically evaluated as a function of the cooling flow, which allowed finding the minimum parameters to ensure efficient and stable cooling. Thus, for the maximum current of 250 A, the parameters of the water-cooling system indicate a required flow of 1-3 l at a cooling water pressure of 5 bar at 25 °C.

ACKNOWLEDGMENT

The authors acknowledge the financial support granted by the Ministry of Research, Digitization, and Innovation through projects PN no. 19310303 / 2019 and PFE 25/2021, which made it possible to carry out this work.

Received on (month day, year)

REFERENCES

1. J. Tanabe, *Iron Dominated Electromagnets Design, Fabrication, Assembly and Measurements* SLAC-R-754 (2005).
2. S. Russenschuck, *Field Computation for Accelerator Magnets*, Wiley – VCH 2010.
3. P. Wang, J. Zheng; Y. Song, W. Zhang, M. Wang, *Analysis and design of an energy verification system for SC200 proton therapy facility*, Electronics, **8**, p. 541 (2019).
4. JS. Zhang, J.X. Zheng, Y.T. Song et al., *Design and field measurement of a dipole magnet for a newly developed superconducting proton cyclotron beamline*, NUCL SCI TECH 29, 133 (2018).
5. K. H. Mess, et al., *Superconducting Accelerator Magnets*, World Scientific (1996).
6. C. K. Yang et al., *Design, Fabrication, and Performance Tests of a HTS Superconducting Dipole Magnet*, IEEE Trans. on Applied Supercond., **22**, *3*, pp. 4000804-4000804, Art no. 4000804 (2012).
7. I. Dobrin, A.M. Morega, D. Enache et al, *High-Temperature Superconductor dipolar magnet for high magnetic field generation – design and fabrication elements*, 10th International Symposium on Advanced Topics in Electrical Engineering, ATEE, Bucharest, Romania, pp. 201-205 (March 23-25).
8. J.D. Jackson, *Classical Electrodynamics*, John Wiley&Sons Inc. (1967).
9. ***Comsol Multiphysics, https://www.comsol.com/
10. ***Luvata, https://www.luvata.com/products